Progress In Electromagnetics Research Letters, Vol. 118, 71-78, 2024

PIER Letters

(Received 24 November 2023, Accepted 4 March 2024, Scheduled 14 March 2024)

The Positive-Definite Stability Analysis for Marching-on-in-Time Schemes

Petrus W. N. van Diepen*, Martijn C. van Beurden, and Roeland J. Dilz

Department of Electrical Engineering, Eindhoven University of Technology, The Netherlands

ABSTRACT: The positive-definite stability analysis (PDSA) is presented as a technique complementary to the companion-matrix stability analysis (CMSA). The PDSA is used to analyze the stability of marching-on-in-time (MOT) schemes. The heart of the PDSA is formed by the analysis on particular linear combinations of interaction matrices from an MOT scheme, which are assumed to be real-valued. If these are all positive definite, then the PDSA guarantees the stability of the scheme. The PDSA can be of a lower complexity than the full CMSA. The construction of the PDSA is shown and applied to two numerical examples.

1. INTRODUCTION

Several spatial-temporal discretizations of the Maxwell equations result in a marching-on-in-time (MOT) scheme, i.e., a scheme where the unknowns at the current time step only depend on the unknowns at previous time steps [1]. Examples are the spatial-temporal discretization of the time domain surface [1–6] and volume [7, 8] integral equations, abbreviated as TDSIE and TDVIE, respectively. To test the stability of the resulting MOT-scheme, i.e., whether its solution remains bounded as the number of time steps goes to infinity, it is common to run the simulation for a large number of time steps and observe either an exponential increase or decrease of the solution. However, this does not demonstrate stability. Performing the companion-matrix stability analysis (CMSA) [2–8] is a way to demonstrate stability for a MOT-scheme. This stability analysis requires the eigenvalue decomposition of the companion matrix for which all eigenvalues have to lie within the unit circle to guarantee stability. The evaluation of the eigenvalues is computationally expensive, as it scales cubically with the dimensions of the companion matrix [9]. In turn, for MOT-schemes based on TDSIEs and TDVIEs, the dimension of the companion matrix scales superlinearly with the number of spatial unknowns [2–8]. Therefore, the CMSA is only used for MOT-schemes with a relatively small number of spatial unknowns. We present a complementary stability analysis in the form of the positive-definite stability analysis (PDSA). The PDSA can have a lower computational complexity than the CMSA, which would enable a stability analysis for MOT-schemes with a higher number of spatial unknowns.

2. COMPANION MATRIX STABILITY ANALYSIS

The companion matrix stability analysis (CMSA) is used to analyze the stability of a marching-on-in-time (MOT) scheme that takes the general form [1–8]

$$\mathbf{Z}_0\mathbf{J}_n = \mathbf{E}^i_n - \sum_{n'=n-\ell}^{n-1} \mathbf{Z}_{n-n'}\mathbf{J}_{n'}, \tag{1}$$

with time step index n at which we intend to compute the unknown vector $\mathbf{J}_n$ based on the solutions for earlier time steps and the excitation vector $\mathbf{E}^i_n$. The interaction matrices $\mathbf{Z}_{n-n'}$ are pre-computed for $n - n' = 0, \ldots, \ell$. The vectors and matrices in the MOT-scheme are of dimension M and $M \times M$, respectively. In the CMSA, we consider the system without exterior excitation, i.e., $\mathbf{E}^i_n = \mathbf{0}$ in Equation (1). In a stable MOT-scheme the $\mathbf{J}_n$ should go to zero for $n \to \infty$. The relation between consecutive solutions $\mathbf{J}_n$ is defined by the companion matrix [2, 5]

$$\mathcal{Q} = \begin{bmatrix} \mathbf{Q}_1 & \mathbf{Q}_2 & \cdots & \mathbf{Q}_{\ell-1} & \mathbf{Q}_\ell \\ \mathbf{I} & \mathbf{0} & \cdots & \mathbf{0} & \mathbf{0} \\ \mathbf{0} & \mathbf{I} & \ddots & \vdots & \vdots \\ \vdots & \ddots & \ddots & \mathbf{0} & \mathbf{0} \\ \mathbf{0} & \cdots & \mathbf{0} & \mathbf{I} & \mathbf{0} \end{bmatrix}. \tag{2}$$

The companion matrix is of dimension $\ell M \times \ell M$ and consists of the $M \times M$ matrix blocks

$$\mathbf{Q}_\ell = -\mathbf{Z}_0^{-1}\mathbf{Z}_\ell. \tag{3}$$

The solution of the unexcited system is bounded if all companion matrix eigenvalues, λ, satisfy $|\lambda| < 1$ or if $|\lambda| = 1$ the algebraic multiplicity is equal to the geometric multiplicity [2, 5]. The computational complexity, i.e., the number of floating-point operations, of obtaining these eigenvalues scales as $\mathcal{O}(\ell^3 M^3)$ [9]. We assume that all vector and matrix elements in the MOT-scheme are real-valued.

* Corresponding author: Petrus W. N. van Diepen (p.w.n.v.diepen@tue.nl).

3. COMPLEMENTARY STABILITY ANALYSIS

The polar representation of a complex companion-matrix eigenvalue is $\lambda = Ae^{\mathrm{j}\theta}$. The value A is the eigenvalue modulus, by definition $A \geq 0$, and for a fixed argument of the eigenvalue, i.e., θ, the eigenvalue is somewhere on the semi-infinite line $\lambda(A) = Ae^{\mathrm{j}\theta}$ with $A \geq 0$ in the complex plane, see Figure 1(a). If the eigenvalue with argument θ has modulus smaller than one, i.e., $A < 1$, the eigenvalue is inside the unit circle and the part of the solution generated by this eigenvalue remains bounded as time goes to infinity. Introducing the coordinate transformation $A = 1 + \alpha$ as illustrated in Figure 1(b), the stability condition becomes $\alpha \in \mathbb{R}^-$, where $\mathbb{R}^-$ is the set of all negative real numbers. The values of $\alpha < -1$, i.e., a negative modulus $A < 0$, are covered in the analysis by changing the argument of analysis from θ to $\theta + \pi$. The values of $\alpha \in \mathbb{C}\backslash\mathbb{R}$ are covered in the analysis by changing the argument of analysis to a different value for θ.

We proceed by making a link between the companion-matrix eigenvalues λ and the real-valued roots of a to-be-constructed polynomial in α. The polynomial in α has coefficients that are composed of weighted linear combinations of interaction matrices. We analyze the positive definiteness of these weighted linear combinations and derive a set of sufficient conditions for stability. Hence, we refer to this procedure as the positive-definite stability analysis (PDSA).

3.1. Construction of a Polynomial in α

To construct a polynomial in α to determine whether CMSA eigenvalues with argument θ satisfy the condition $\alpha \in \mathbb{R}^-$, we consider the matrix polynomial represented by the eigenvalue and eigenvector pair, λ and $\mathbf{v}_{\mathcal{Q}}$. The eigenvector $\mathbf{v}_{\mathcal{Q}}$ is of dimension ℓM. Each λ-$\mathbf{v}_{\mathcal{Q}}$ pair of the companion matrix in Equation (2) has to satisfy the eigenvalue-eigenvector relation [10]

$$(\mathcal{Q} - \lambda\mathbf{I})\,\mathbf{v}_{\mathcal{Q}} = \begin{bmatrix} \mathbf{Q}_1 - \lambda\mathbf{I} & \mathbf{Q}_2 & \mathbf{Q}_3 & \cdots & \mathbf{Q}_{\ell-1} & \mathbf{Q}_\ell \\ \mathbf{I} & -\lambda\mathbf{I} & \mathbf{0} & \cdots & \mathbf{0} & \mathbf{0} \\ \mathbf{0} & \mathbf{I} & -\lambda\mathbf{I} & \ddots & \vdots & \vdots \\ \vdots & \ddots & \ddots & \ddots & \mathbf{0} & \mathbf{0} \\ \vdots & & \ddots & \ddots & -\lambda\mathbf{I} & \mathbf{0} \\ \mathbf{0} & \cdots & \cdots & \mathbf{0} & \mathbf{I} & -\lambda\mathbf{I} \end{bmatrix} \mathbf{v}_{\mathcal{Q}} = \mathbf{0}. \tag{4}$$

Each block row in the above equation, apart from the first one, has an $-\lambda\mathbf{I}$ block after the block $\mathbf{I}$, which enforces a scaling by λ between the ℓ consecutive blocks of $\mathbf{v}_{\mathcal{Q}}$, i.e., $\mathbf{v}_{\mathcal{Q}}$ has the following structure

$$\mathbf{v}_{\mathcal{Q}} = \left[\lambda^{\ell-1}\mathbf{v}, \lambda^{\ell-2}\mathbf{v}, \ldots, \lambda\mathbf{v}, \mathbf{v}\right]^T, \tag{5}$$

where ^{T} denotes the transpose. We refer to $\mathbf{v}$ as the sub-eigenvector of the companion matrix, which is of dimension M. Consequently, the partitioning of $\mathbf{v}_{\mathcal{Q}}$ in Equation (5) automatically satisfies all the block rows in (4), except for the first one. Thus, $\mathbf{v}$ still has to satisfy

$$\left[\lambda^{\ell-1}(\mathbf{Q}_1 - \lambda\mathbf{I}) + \lambda^{\ell-2}\mathbf{Q}_2 + \ldots + \lambda\mathbf{Q}_{\ell-1} + \mathbf{Q}_\ell\right]\mathbf{v} = \mathbf{0}. \tag{6}$$

Substitution of Equation (3) in the above equation results in

$$[\lambda^\ell\mathbf{Z}_0 + \lambda^{\ell-1}\mathbf{Z}_1 + \lambda^{\ell-2}\mathbf{Z}_2 + \ldots + \lambda\mathbf{Z}_{\ell-1} + \mathbf{Z}_\ell]\mathbf{v} = \mathbf{0}. \tag{7}$$

The eigenvalues $\lambda = (1+\alpha)e^{\mathrm{j}\theta}$ on the pertaining line in Figure 1(b) then yield, via the binomial theorem,

$$\lambda^\ell = (1+\alpha)^\ell e^{\mathrm{j}\ell\theta} = e^{\mathrm{j}\ell\theta}\sum_{k=0}^{\ell}\binom{\ell}{k}\alpha^k. \tag{8}$$

Substitution of this expression in (7) and grouping terms of equal power in α yields

$$\begin{aligned} &\Big[\alpha^\ell\mathbf{Z}_0 + \alpha^{\ell-1}\left\{\ell\mathbf{Z}_0 + e^{-\mathrm{j}\theta}\mathbf{Z}_1\right\} \\ &+\alpha^{\ell-2}\left\{\binom{\ell}{\ell-2}\mathbf{Z}_0 + (\ell-1)e^{-\mathrm{j}\theta}\mathbf{Z}_1 + e^{-\mathrm{j}2\theta}\mathbf{Z}_2\right\} \\ &+\ldots \\ &+\alpha\left\{\ell\mathbf{Z}_0 + (\ell-1)e^{-\mathrm{j}\theta}\mathbf{Z}_1 + \ldots + e^{-\mathrm{j}(\ell-1)\theta}\mathbf{Z}_{\ell-1}\right\} \\ &+\left\{\mathbf{Z}_0 + e^{-\mathrm{j}\theta}\mathbf{Z}_1 + \ldots + e^{-\mathrm{j}(\ell-1)\theta}\mathbf{Z}_{\ell-1} + e^{-\mathrm{j}\ell\theta}\mathbf{Z}_\ell\right\}\Big]\mathbf{v} = \mathbf{0}. \end{aligned} \tag{9}$$

We have now obtained a complex-valued matrix polynomial in α. Pre-multiplication of (9) by the conjugate transpose of $\mathbf{v}$ with phase offset ϕ, i.e., $e^{-\mathrm{j}\phi}\mathbf{v}^H$ with ^{H} denoting the conjugate transpose, yields a polynomial in α with complex scalar coefficients, i.e.

$$\begin{aligned} &\alpha^\ell\mathbf{v}^H e^{-\mathrm{j}\phi}\mathbf{Z}_0\mathbf{v} + \alpha^{\ell-1}\mathbf{v}^H\left\{\ell e^{-\mathrm{j}\phi}\mathbf{Z}_0 + e^{-\mathrm{j}+(\theta+\phi)}\mathbf{Z}_1\right\}\mathbf{v} + \\ &\alpha^{\ell-2}\mathbf{v}^H\left\{\binom{\ell}{\ell-2}e^{-\mathrm{j}\phi}\mathbf{Z}_0 + (\ell-1)e^{-\mathrm{j}(\theta+\phi)}\mathbf{Z}_1 + e^{-\mathrm{j}(2\theta+\phi)}\mathbf{Z}_2\right\}\mathbf{v} + \\ &\ldots + \\ &\alpha\mathbf{v}^H\left\{\ell e^{-\mathrm{j}\phi}\mathbf{Z}_0 + (\ell-1)e^{-\mathrm{j}(\theta+\phi)}\mathbf{Z}_1 + \ldots + e^{-\mathrm{j}((\ell-1)\theta+\phi)}\mathbf{Z}_{\ell-1}\right\}\mathbf{v} + \\ &\mathbf{v}^H\left\{e^{-\mathrm{j}\phi}\mathbf{Z}_0 + e^{-\mathrm{j}(\theta+\phi)}\mathbf{Z}_1 + \ldots + e^{-\mathrm{j}((\ell-1)\theta+\phi)}\mathbf{Z}_{\ell-1} + e^{-\mathrm{j}(\ell\theta+\phi)}\mathbf{Z}_\ell\right\}\mathbf{v} \\ &= 0, \end{aligned} \tag{10}$$

where each coefficient consists of a weighted sum of interaction matrices with a still free-to-choose parameter ϕ.

3.2. Cornerstone of the PDSA: Descartes' Rule of Signs

In Equation (10) we obtained a polynomial in α with complex scalar coefficients. Unfortunately, not much can be said about the solutions of such polynomials. However, if we obtain a polynomial in α with real-valued scalar coefficients, we can apply Descartes' rule of signs [11], which states that the real-valued roots of a polynomial equation all satisfy $\alpha \in \mathbb{R}^-$, if the real-valued scalar coefficients all have equal sign. To obtain a polynomial in α with the same real-valued roots as Equation (10), but now with real-valued scalar coefficients, we use the fact that a polynomial with conjugated coefficients has the same real-valued roots. So, adding two polynomials with complex conjugated polynomial coefficients, results in a polynomial with the same real-valued roots, but with real-valued polynomial coefficients. Thus, the following polynomial has the same real-valued roots as the polynomial in Equation (10)

$$\begin{aligned} &\alpha^\ell\mathbf{v}^H\left\{e^{-\mathrm{j}\phi}\mathbf{Z}_0\right\}^S\mathbf{v} + \alpha^{\ell-1}\mathbf{v}^H\left\{\ell e^{-\mathrm{j}\phi}\mathbf{Z}_0 + e^{-\mathrm{j}(\theta+\phi)}\mathbf{Z}_1\right\}^S\mathbf{v} + \\ &\alpha^{\ell-2}\mathbf{v}^H\left\{\binom{\ell}{\ell-2}e^{-\mathrm{j}\phi}\mathbf{Z}_0 + (\ell-1)e^{-\mathrm{j}(\theta+\phi)}\mathbf{Z}_1 + e^{-\mathrm{j}(2\theta+\phi)}\mathbf{Z}_2\right\}^S\mathbf{v} + \end{aligned}$$

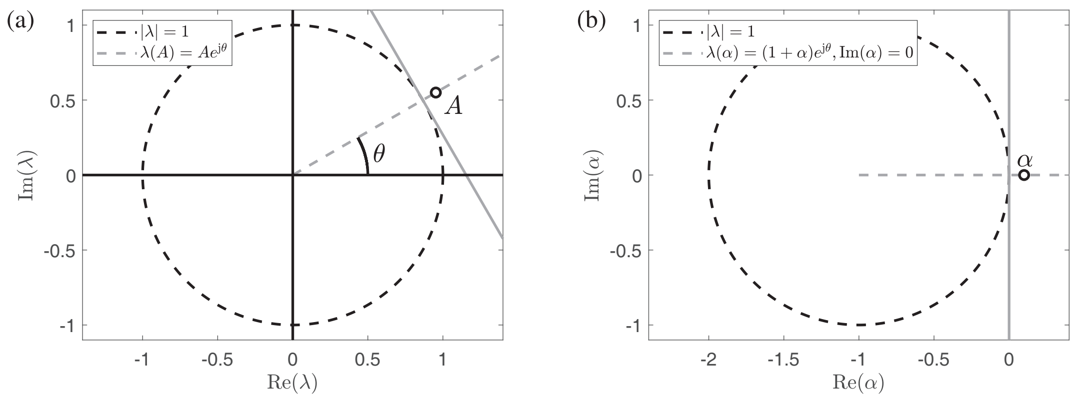

FIGURE 1. (a) We limit the CMSA to the eigenvalues with argument θ represented by the line $\lambda(A) = Ae^{j\theta}$ with modulus $A \geq 0$. The part of the solution generated by these eigenvalues are bounded as the number of time steps goes to infinity if we can prove that $A < 1$. (b) The figure shown in (a) but under the coordinate transformation $A = 1+\alpha$. The eigenvalues on $\lambda(A) = Ae^{j\theta}$ with $A \geq 0$ are represented by $\lambda(\alpha) = (1+\alpha)e^{j\theta}$ with $\alpha \in \mathbb{R}$. The stability condition then becomes $\alpha \in \mathbb{R}^-$. The values $\alpha < -1$, i.e., a negative modulus $A < 0$, are covered in the analysis by changing the argument of analysis θ to $\theta + \pi$. The values of $\alpha \in \mathbb{C}\backslash\mathbb{R}$, are covered in the analysis by changing the argument of analysis to a different θ.

$$\begin{aligned}&\ldots+\\&\alpha\mathbf{v}^H\left\{\ell e^{-j\phi}\mathbf{Z}_0+(\ell-1)e^{-j(\theta+\phi)}\mathbf{Z}_1+\ldots+e^{-j((\ell-1)\theta+\phi)}\mathbf{Z}_{\ell-1}\right\}^S\mathbf{v}+\\&\mathbf{v}^H\left\{e^{-j\phi}\mathbf{Z}_0+e^{-j(\theta+\phi)}\mathbf{Z}_1+\ldots+e^{-j((\ell-1)\theta+\phi)}\mathbf{Z}_{\ell-1}+e^{-j(\ell\theta+\phi)}\mathbf{Z}_\ell\right\}^S\mathbf{v}\\&=0,\end{aligned}\tag{11}$$

where ^{S} denotes the symmetric part of the matrix, e.g., $\left\{e^{-j\phi}\mathbf{Z}_0\right\}^S = \frac{1}{2}(e^{-j\phi}\mathbf{Z}_0 + e^{j\phi}\mathbf{Z}_0^H)$. This polynomial in α has polynomial coefficients of the form $\mathbf{v}^H\mathbf{D}_n\mathbf{v}$, where $\mathbf{D}_n$ represents the symmetric part of the weighted sum of interaction matrices belonging to $\alpha^{\ell-n}$, which are of the following form

$$\begin{aligned}\mathbf{D}_n(\theta,\phi) &= \binom{\ell}{\ell-n}\left\{e^{-j\phi}\mathbf{Z}_0\right\}^S+\binom{\ell-1}{\ell-n}\left\{e^{-j(\theta+\phi)}\mathbf{Z}_1\right\}^S+\\&\ldots+\binom{\ell-n}{\ell-n}\left\{e^{-j(n\theta+\phi)}\mathbf{Z}_n\right\}^S.\end{aligned}\tag{12}$$

As the symmetric part of a matrix is always Hermitian [10], the polynomial coefficients $\mathbf{v}^H\mathbf{D}_n\mathbf{v}$ are real, and we can apply Descartes' rule of signs. If $\mathbf{D}_n$ is positive definite, i.e., $\mathbf{v}^H\mathbf{D}_n\mathbf{v} > 0$ for any nonzero $\mathbf{v} \in \mathbb{C}$, for all n, then the real-valued polynomial coefficients in Equation (11) are all positive, irrespective of $\mathbf{v}$. So, even though we use $\mathbf{v}$ in the construction of the polynomial in Equation (11), we do not need to compute it.

3.3. Positive-Definite Stability Analysis (PDSA)

At the start of Section 3, we found that the companion matrix eigenvalues with argument θ have a modulus smaller than one, i.e., lie within the unit circle, if $\alpha \in \mathbb{R}^-$. In the preceding section, we have shown that Descartes' rule of signs guarantees $\alpha \in \mathbb{R}^-$ if there is a value of ϕ for which each matrix $\mathbf{D}_n(\theta, \phi)$ in (12) is positive definite for $n = 0, \ldots, \ell$. Combined, we can formulate the positive-definite stability analysis (PDSA) as: a sufficient condition for the companion-matrix eigenvalues with argument θ to have a modulus smaller than one, i.e., lie within the unit circle, is that all matrices $\mathbf{D}_n(\theta, \phi)$ as defined in Equation (12) are positive definite.

For $\theta = 0$ and $\theta = \pi$, the PDSA is further simplified. As the interaction matrices are real, the companion matrix is too, so are the sub-eigenvectors $\mathbf{v}$ pertaining to these arguments θ [10]. Therefore, we can factorize the $e^{-j\phi}$ out of all the polynomial coefficients in Equation (11), i.e., $\mathbf{v}^H\mathbf{D}_n(\theta, \phi)\mathbf{v} = \cos(\phi)\mathbf{v}^T\mathbf{D}_n(\theta, 0)\mathbf{v}$ for $\theta \in \{0, \pi\}$. Thus, we can set ϕ to zero.

It is possible that $\mathbf{D}_\ell$ (12) has a null space independent of ϕ, i.e., $\mathbf{D}_\ell(\theta, \phi)\mathbf{v} = \mathbf{0}$ for $\mathbf{v} \neq \mathbf{0}$ for all ϕ. In that case, the pertaining polynomial in α has the solution $\alpha = 0$ with a multiplicity equal to the dimension of the null space of $\mathbf{D}_\ell$. This implies that a number of eigenvalues is positioned on the unit circle at $\lambda = e^{j\theta}$ with algebraic multiplicity equal to the dimension of the null space of $\mathbf{D}_\ell$. The part of the solution generated by these eigenvalues is only bounded if the geometric multiplicity is equal to the algebraic multiplicity [5, 10].

4. NUMERICAL EXAMPLES

4.1. Second-Order Ordinary Differential Equation

We illustrate the use of the PDSA using the following second-order ordinary differential equation (ODE)

$$\frac{\mathrm{d}y^2}{\mathrm{d}t^2} + p\frac{\mathrm{d}y}{\mathrm{d}t} + y = E(t),\tag{13}$$

with initial conditions $y(t) = 0$ and $\frac{\mathrm{d}}{\mathrm{d}t}y(t) = 0$ for $t \leq 0$ and excitation function $E(t) = t$ for $0 \leq t \leq 1$ and zero elsewhere.

The Green function pertaining the ODE (13) for $|p| < 2$ subject to the initial conditions is given by

$$G(t-t') = \frac{1}{\sqrt{1-\frac{p^2}{4}}}e^{-\frac{p}{2}(t-t')}\sin\left(\sqrt{1-\frac{p^2}{4}}(t-t')\right)H(t-t'),\tag{14}$$

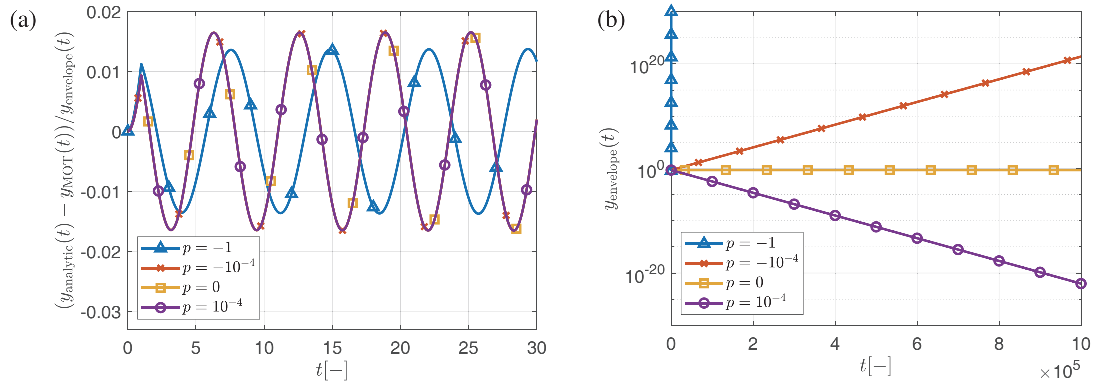

FIGURE 2. (a) The difference between the analytic solution $y_{\text{analytic}}(t)$ based on the Green function in Equation (14) and the MOT-scheme solution $y_{\text{MOT}}(t)$ from Equation (15) with $\Delta t = 10^{-2}$, normalized to the envelope of the solution, $y_{\text{envelope}}(t)$ shown in (b), for different values of p. (b) The envelope $y_{\text{envelope}}(t)$ of the analytic and MOT-scheme solution for a long simulation.

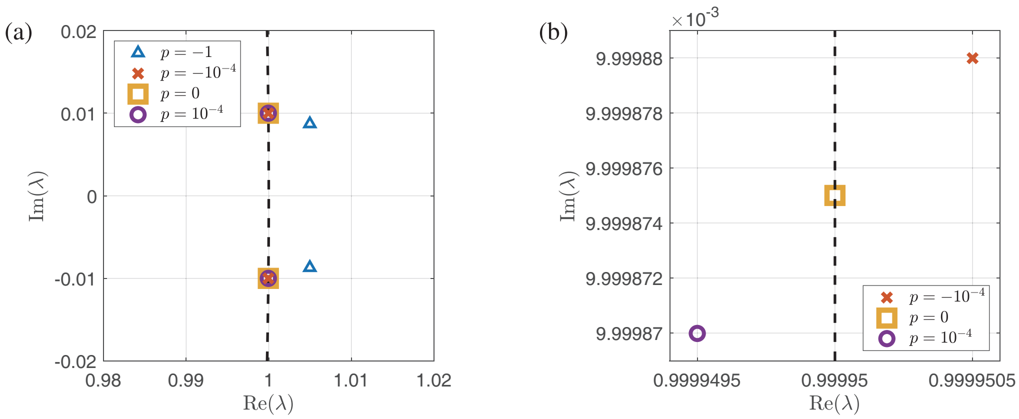

FIGURE 3. The black dashed line indicates the unit circle in the complex plane, i.e., $|\lambda| = 1$. (a) The companion matrix eigenvalues λ belonging to the MOT-scheme from Equation (15) for different values of p. (b) Zoom-in of the eigenvalues in (a).

with $H(t-t')$ the Heaviside step function. The solution $y(t)$ is found by convolution between the Green function and the excitation function, i.e., $y_{\text{analytic}}(t) = \int G(t-t')E(t')\mathrm{d}t'$.

Instead of finding the analytic solution to Equation (13), we approximate the first- and second-order derivatives of the ODE by the first- and second-order central finite difference approximations, such that we arrive at the recurrence relation

$$\mathbf{Z}_0 y_{\text{MOT}}((n+1)\Delta t) + \mathbf{Z}_1 y_{\text{MOT}}(n\Delta t) + \mathbf{Z}_2 y_{\text{MOT}}((n-1)\Delta t) = E(n\Delta t), \tag{15}$$

for $n \geq 1$, to obtain a MOT-scheme of the form (1) in which the interaction matrices are now scalars, i.e., $M = 1$, with $\mathbf{Z}_0 = \left(\frac{1}{\Delta t^2} + \frac{p}{2\Delta t}\right)$, $\mathbf{Z}_1 = \left(1 - \frac{2}{\Delta t^2}\right)$ and $\mathbf{Z}_2 \left(\frac{1}{\Delta t^2} - \frac{p}{2\Delta t}\right)$. We set $\Delta t = 10^{-2}$ and compare the MOT-scheme and analytic solutions for different values of p, i.e., $p \in \{-1, -10^{-4}, 0, 10^{-4}\}$.

The absolute difference between the analytic and MOT-scheme solutions, normalized to the envelope of the solutions, is shown in Figure 2(a), and it illustrates that the MOT-scheme approximates the oscillations of the analytic solution up to an accuracy of 0.02 with respect to the peaks in the first three thousand time steps of the simulation. Continuing the simulation up to $t = 10^6$, the envelope is shown in Figure 2(b). We conclude that $p = 10^{-4}$ will exponentially decrease over time; $p = 0$ oscillates forever; and $p = -10^{-4}$ and $p = -1$ will increase exponentially over time. We will use the PDSA as defined in Section 3.3 and compare these to the results shown in Figure 2(b).

We start by computing the eigenvalue arguments θ. In Figure 3 we plot the companion matrix eigenvalues λ. We use these eigenvalues to determine θ for each p. The eigenvalues for $p \in \{10^{-4}, 0, -10^{-4}\}$ are closely spaced together, see Figure 3(b), and the difference between the arguments is in the order of 10^{-10}. As we have defined θ for each value of the parameter p in (13), we can compute the matrices $\mathbf{D}_n(\theta, \phi)$ (12) for $n = 0, 1, 2$ and check whether there is a value of ϕ for which all matrices are positive definite. In this numerical example, the matrices are scalars, i.e., $M = 1$, so the matrix is positive definite if the corresponding scalar is larger than zero. We start with the positive definiteness of $\mathbf{D}_0(\theta, \phi) = \{e^{-\mathrm{j}\phi}\mathbf{Z}_0\}^S$. The interaction matrix $\mathbf{Z}_0$ is symmetric as it is a scalar, thus we can rewrite the expression as $\mathbf{D}_0(\theta, \phi) = \cos(\phi)\mathbf{Z}_0$. As long as $\mathbf{Z}_0$ is positive definite, then so is $\mathbf{D}_0(\theta, \phi)$ for $-\frac{\pi}{2} < \phi < \frac{\pi}{2}$, which limits the feasible values of ϕ. The values of the matrices $\mathbf{D}_n(\theta, \phi)$ with $-\frac{\pi}{2} < \phi < \frac{\pi}{2}$ for $n = 1$ and $n = 2$ are shown in Figure 4. The areas marked in these figures indicate the regions where $\mathbf{D}_n(\theta, \phi) < 0$.

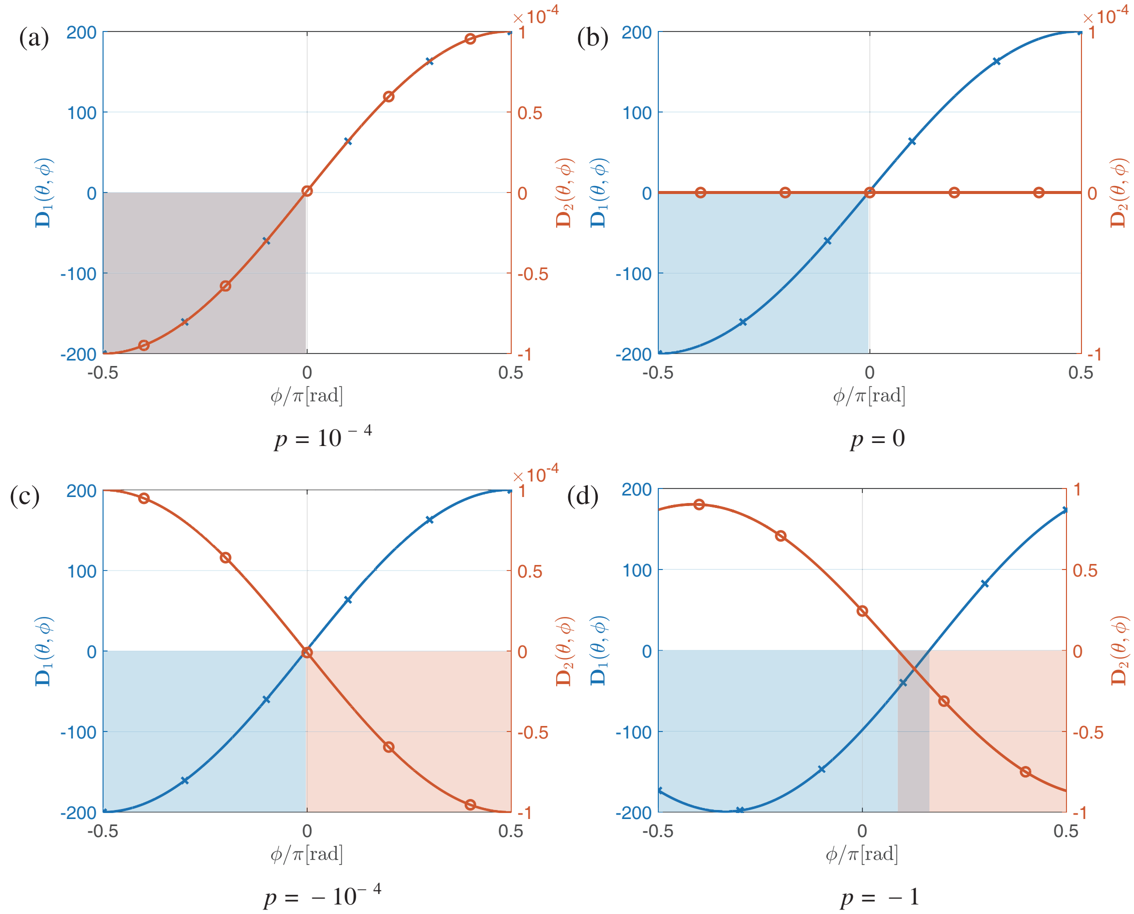

FIGURE 4. The PDSA for the MOT-scheme in Equation (15) which depends on p requires us to compute the eigenvalues of the matrices $\mathbf{D}_n(\theta, \phi)$ defined in Equation (12) for a range of ϕ. As the matrices are scalars their eigenvalues correspond to the matrix value. The left (blue) and right (orange) y-axis show $\mathbf{D}_1(\theta, \phi)$ and $\mathbf{D}_2(\theta, \phi)$, respectively. The blue and orange areas marked in (a)–(d) mark the areas where $\mathbf{D}_1(\theta, \phi) < 0$ and $\mathbf{D}_2(\theta, \phi) < 0$, respectively. If the blue and orange area overlap, the area is marked as gray.

In the case $p = 10^{-4}$, we can find a range of values for ϕ in Figure 4(a) for which $\mathbf{D}_n(\theta, \phi) > 0$ for $n = 1$ and $n = 2$. Then, according to the PDSA, that is a sufficient condition for the companion matrix eigenvalues with argument θ to have a modulus smaller than one, i.e., within the unit circle. Thus, the associated solution is bounded. This is in line with the results shown in Figure 3(b), where the pertaining eigenvalue is inside the unit circle, and the solution envelope in Figure 2(b), which is bounded.

In the case $p = 0$, the matrix $\mathbf{D}_1(\theta, \phi)$ in Figure 4(b) has a dimension one null space independent of ϕ, i.e., as the matrix $\mathbf{D}_1(\theta, \phi)$ is a scalar, it is zero up to the finite precision of the calculation for all ϕ. Then, according to the PDSA, there is a single companion matrix eigenvalue at $\lambda = e^{j\theta}$. This is in line with the results shown in Figure 3(b), where the pertaining eigenvalue lies on the unit circle. Since there is only a single eigenvalue in Figure 3(b) at $e^{j\theta}$ and a complex conjugate in Figure 3(a), the pertaining solution is a pure oscillation, in line with the solution envelope shown in Figure 2(b).

In the cases $p = -10^{-4}$, see Figure 4(c), and $p = -1$, see Figure 4(d), the matrices $\mathbf{D}_1(\theta, \phi)$ and $\mathbf{D}_2(\theta, \phi)$ are not positive definite in the blue and orange marked regions, respectively. Since these regions overlap, although barely in Figure 4(c), there is no ϕ for which the matrices $\mathbf{D}_n(\theta, \phi)$ are positive definite and the PDSA does not give a sufficient condition for the companion matrix eigenvalues to be within the unit circle. This is in line with the results shown in Figure 3(a) as the pertaining eigenvalues have left the unit circle.

4.2. MOT-TDEFIE Stabilization

The MOT-TDEFIE is a spatial-temporal discretization of the time-differentiated time domain electric field integral equation (TDEFIE) [3–6] that results in a MOT-scheme of the form given in Equation (1). The MOT-TDEFIE can be used to simulate for example the surface current density on a perfect electric conductive (PEC) $2 \times 2\,\mathrm{m}^2$ plate induced by a Gaussian plane wave, as in Section 3 of [6]. As can be seen in Figure 5 in [6], the MOT-TDEFIE suffers from late-time instability. The pertaining unbounded solution is first observed as linear-in-time, but the analysis in [5] predicts an exponential increase after approximately a hundred million time steps. This prediction is based on companion-matrix eigenvalues pertaining the MOT-TDEFIE interaction matrices. A part of these eigenvalues are clustered around $\lambda = 1$, where half of this cluster resides out-

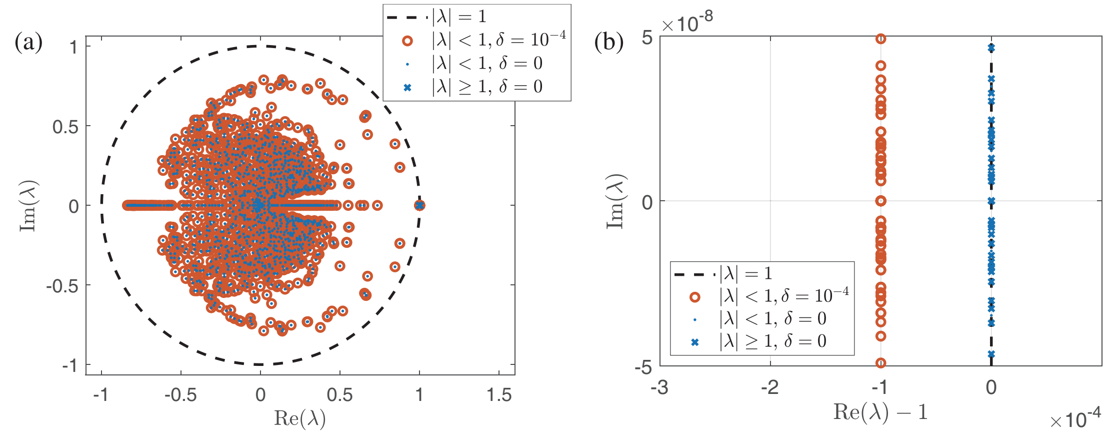

FIGURE 5. (a) The companion matrix eigenvalues λ pertaining to the MOT-TDEFIE used in Section 3 of [6]. (b) A zoom-in at the eigenvalues around $\lambda = 1$.

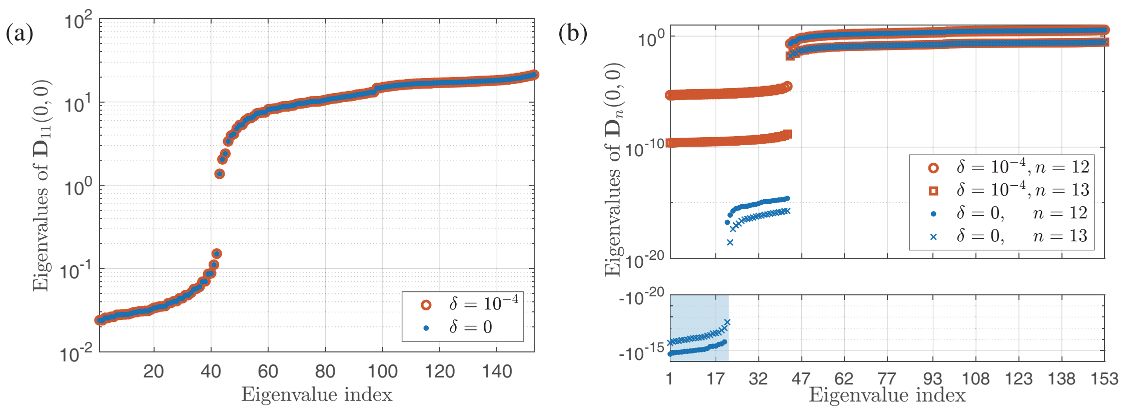

FIGURE 6. The eigenvalues of the matrix $\mathbf{D}_n(0,0)$ (12) for (a) $n = 11$, (b) $n = 12$ and $n = 13$ constructed from the MOT-TDEFIE interaction matrices used in Section 3 of [6] with stabilization ($\delta = 10^{-4}$) and without stabilization ($\delta = 0$). The blue area marks the region where some eigenvalues of $\mathbf{D}_{12}(0,0)$ and $\mathbf{D}_{13}(0,0)$ are smaller than zero, in the case without stabilization ($\delta = 0$).

side the unit circle. These eigenvalues outside the unit circle cause the aforementioned instability in the MOT-TDEFIE. In [6], a technique was presented to move this cluster of eigenvalues by a predefined value δ to the interior of the unit circle. Consequently, this moves the eigenvalues outside the unit circle to the inside of the unit circle, therefore stabilizing the MOT-TDEFIE.

To illustrate this stabilization technique, we have computed the eigenvalues pertaining to the numerical experiment in Section 3 of [6] without a shift, $\delta = 0$, and with a shift, $\delta = 10^{-4}$. The eigenvalues are plotted in Figure 5(a) and we zoom in at $\lambda = 1$ in Figure 5(b). Half of the cluster of eigenvalues around $\lambda = 1$ for $\delta = 0$ in Figure 5(b) is indeed outside the unit circle and the whole cluster of eigenvalues is shifted $\delta = 10^{-4}$ to the inside of the unit circle. Consequently, all eigenvalues are in the interior of the unit circle, see Figure 5(a) and the pertaining solution remains bounded for a number of time steps approaching infinity, see Figure 5 in [6].

The dimension $M \times M$ of the MOT-TDEFIE interaction matrices $\mathbf{Z}_{n-n'}$ for $n - n' = 0, \ldots, \ell$ is equal to the number of spatial basis functions used to discretize the unknown surface current density [1–6]. The number of interaction matrices for MOT-TDEFIE is proportional to the square root of M, i.e., $\ell \sim \mathcal{O}(\sqrt{M})$ [1–6]. The computational complexity of the CMSA for MOT-TDEFIE is then $\mathcal{O}(M^{\frac{9}{2}})$, which severely limits the value for M. We analyze the MOT-TDEFIE stabilization technique presented in [6] with the PDSA presented in Section 3.3.

We start by setting $\theta = 0$, since part of the cluster of companion-matrix eigenvalues is on the positive real axis, see Figure 5(b). As $\theta = 0$, the PDSA simplifies and we only have to perform the analysis for $\phi = 0$. The MOT-TDEFIE used in Section 3 of [6] consists of fourteen interaction matrices, i.e., $\ell = 13$, so we have to analyze the positive-definiteness of $\mathbf{D}_n(0,0)$ (12) for $n = 0, \ldots, 13$, i.e., compute the eigenvalues of $\mathbf{D}_n(0,0)$ and determine if they are all larger than zero. The matrices with and without stabilization up to $n = 11$ are found to be all positive-definite, e.g., the eigenvalues of $\mathbf{D}_{11}(0,0)$ shown in Figure 6(a) are all larger than zero. The matrices $\mathbf{D}_{12}(0,0)$ and $\mathbf{D}_{13}(0,0)$ without stabilization are indefinite, as some of the eigenvalues of $\mathbf{D}_{12}(0,0)$ and $\mathbf{D}_{13}(0,0)$ are negative, i.e., the eigenvalues in the blue shaded area at the bottom-left in Figure 6(b). It is not surprising that the issue is related to the matrices $\mathbf{D}_{12}(0,0)$

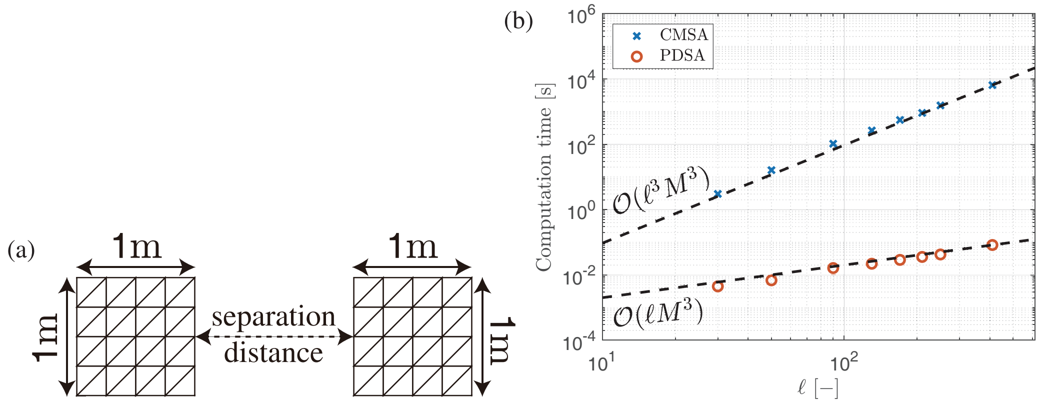

FIGURE 7. (a) Two meshed $1\,\mathrm{m}^2$ PEC plates separated by a distance that is increased to increase ℓ, i.e., the number of interaction matrices in the MOT-TDEFIE, for fixed $M = 80$, i.e., the number of spatial basis functions. (b) The computation time required to compute the CMSA eigenvalues and the eigenvalues of $\mathbf{D}_n(0,0)$ (12) for $n = 0, \ldots, \ell$ in the PDSA corresponding to the configuration shown in (a).

and $\mathbf{D}_{13}(0,0)$, as these can be represented as $\mathbf{D}_{12}(0,0)\mathbf{v} = [\mathbf{Z}_0, \mathbf{Z}_1, \mathbf{Z}_2, \ldots, \mathbf{Z}_{11}, \mathbf{Z}_{\ell-1}, \mathbf{Z}_\ell][13\mathbf{v}, 12\mathbf{v}, 11\mathbf{v}, \ldots, 2\mathbf{v}, \mathbf{v}, \mathbf{0}]^T$, i.e., a matrix-vector product of the interaction matrices and a solution vector that increases linearly in time, and $\mathbf{D}_\ell(0,0)\mathbf{v} = [\mathbf{Z}_0, \mathbf{Z}_1, \mathbf{Z}_2, \ldots, \mathbf{Z}_{\ell-2}, \mathbf{Z}_{\ell-1}, \mathbf{Z}_\ell][\mathbf{v}, \mathbf{v}, \mathbf{v}, \ldots, \mathbf{v}, \mathbf{v}, \mathbf{v}]^T$, i.e., a matrix-vector product of the interaction matrices and a solution vector that is constant in time. Both the linear-in-time and constant-in-time solutions are in the null space of the TDEFIE [5]. As the matrices $\mathbf{D}_{12}(0,0)$ and $\mathbf{D}_{13}(0,0)$ without stabilization are indefinite, the PDSA does not offer a sufficient condition for the companion matrix eigenvalues with argument $\theta = 0$, i.e., those on the positive real axis, to be within the unit circle. This is in line with the results shown in Figures 5(a) and 5(b), as eigenvalues appear on the positive real axis outside the unit circle. On the contrary, after applying the stabilization, the matrices $\mathbf{D}_{12}(0,0)$ and $\mathbf{D}_{13}(0,0)$ are positive-definite, i.e., the eigenvalues of $\mathbf{D}_{12}(0,0)$ and $\mathbf{D}_{13}(0,0)$ in Figure 6(b) are all positive. Now, according to the PDSA in Section 3.3, this is a sufficient condition for the companion matrix eigenvalues with argument $\theta = 0$, i.e., those on the positive real axis, to have a modulus smaller than one and be within the unit circle. This is in line with the results shown in Figures 5(a) and 5(b).

5. DISCUSSION ON USEFULNESS AND LIMITATIONS OF PDSA

In Section 4, we presented two numerical examples where we applied the PDSA. Although these numerical examples illustrate that the PDSA holds for real-valued MOT-schemes, the numerical examples also illustrate some limitations.

In the numerical example of Section 4.1, where $\theta \notin \{0, \pi\}$, we encounter two issues. The first one is related to finding the correct value for θ. We computed these via the CMSA. However, performing this computation makes the PDSA obsolete. Instead, we could estimate θ by performing a simulation and carrying out a Fourier analysis on the MOT-scheme solution, but the argument will never be exactly obtained. The second issue is related to finding a value for ϕ for which all matrices are positive definite. We determine positive-definiteness by computing the eigenvalues of $\mathbf{D}_n(\theta,\phi)$ for $n = 0, \ldots, \ell$. The range of ϕ is normally from $-\pi$ to π, but for MOT-schemes with symmetric interaction matrices, e.g., MOT-TDEFIE in Section 4.2, the range reduces to $-\frac{\pi}{2} < \phi < \frac{\pi}{2}$ as explained in Section 4.1. Still, there is an infinite number of values for ϕ to analyze $\mathbf{D}_n(\theta,\phi)$ for $n = 1, \ldots, \ell$, before we can state there exists no ϕ for which all matrices $\mathbf{D}_n(\theta,\phi)$ are positive definite. Although the eigenvalues $\mathbf{D}_n(\theta,\phi)$ depend continuously on both θ and ϕ [10], which will alleviate both issues a bit, the PDSA has a limited use for the analysis for eigenvalue arguments $0 < \theta < \pi$, since the number of computations is likely to be higher than performing the companion-matrix stability analysis.

However, many of the issues regarding discretizations of time domain integral equations that result in MOT-schemes are related to the companion-matrix eigenvalue arguments $\theta = 0$, e.g., the Jordan blocks in MOT-(TD)EFIE [5,6], or $\theta = \pi$, e.g., the accuracy of the interaction matrices in the MOT-(TD)EFIE [3] or the temporal basis function used to expand the unknown in the discretization of the TDSIE [4] and the TD-VIE [7,8]. If θ is either zero or π, the PDSA only needs to be performed for $\phi = 0$. Therefore, the computational complexity of the PDSA for $\theta = 0$ or $\theta = \pi$ is equal to the computational complexity of computing the eigenvalues of the matrices $\mathbf{D}_n(0,0)$ for $n = 0, \ldots, \ell$, which amounts to $\mathcal{O}(\ell M^3)$ where $M \times M$ is the dimension of each interaction matrix. This is of a lower complexity than the CMSA, which is $\mathcal{O}(\ell^3 M^3)$. We illustrate the respective scaling with the simple numerical experiment in Figure 7(a) of the two PEC plates discretized with $M = 80$ spatial basis functions. We incrementally increase the separation distance between these two PEC plates to increase ℓ without altering M. The computation time required to compute all CMSA eigenvalues and the eigenvalues of $\mathbf{D}_n(0,0)$ (12) for $n = 0, \ldots, \ell$ in the PDSA is plotted in Figure 7(b) as a function of ℓ. The CMSA and PDSA are implemented with MATLAB R2019a running on Intel(R) Core(TM) i7-9750H CPU @ 2.60 GHz. In Figure 7(b), we numerically verify the superior complexity scaling of the PDSA compared to the CMSA. Thus, the PDSA is useful for MOT-schemes if one is interested in the positive and negative real-valued companion-matrix eigenvalues, i.e., the boundedness towards infinity of monotonic or per-time-step-alternating solutions, respectively.

6. CONCLUSION

We have presented the positive definite stability analysis (PDSA) as a technique complementary to the companion matrix stability analysis (CMSA). We have shown the construction of the PDSA and applied it to two numerical examples. The heart of the PDSA is formed by the analysis on particular linear combinations of interaction matrices from an MOT scheme, which are assumed to be real-valued. If these are all positive definite, then the PDSA guarantees the stability of the scheme. The PDSA is most useful if one is interested in the boundedness of the monotonically behaving solutions or the per-time-step-alternating solutions, i.e., the solutions pertaining to the positive and negative real-valued eigenvalues of the companion matrix, respectively, as the computational complexity of the PDSA is then lower than that of the full CMSA.

REFERENCES

[1] Poggio, A. J. and E. K. Miller, *Integral Equation Solutions of Three-dimensional Scattering Problems*, 1st ed., 159–264, Pergamon Press, 1973.

[2] Dodson, S. J., "Implicitness and stability of time domain integral equation scattering analyses," *The Applied Computational Electromagnetics Society Journal (ACES)*, 291–301, 1998.

[3] Van't Wout, E., D. R. v. d. Heul, H. v. d. Ven, and C. Vuik, "The influence of the exact evaluation of radiation fields in finite precision arithmetic on the stability of the time domain integral equation method," *IEEE Transactions on Antennas and Propagation*, Vol. 61, No. 12, 6064–6074, Dec. 2013.

[4] Van't Wout, E., D. R. v. d. Heul, H. v. d. Ven, and C. Vuik, "Stability analysis of the marching-on-in-time boundary element method for electromagnetics," *Journal of Computational and Applied Mathematics*, Vol. 294, 358–371, Mar. 2016.

[5] Van Diepen, P. W. N., R. J. Dilz, A. P. M. Zwamborn, and M. C. v. Beurden, "The role of jordan blocks in the MOT-scheme time domain EFIE linear-in-time solution instability," *Progress In Electromagnetics Research B*, Vol. 95, 123–140, 2022.

[6] Van Diepen, P. W. N., R. J. Dilz, and M. C. v. Beurden, "Jordan block eigenvalue shift in the marching-on-in-time electric field integral equation," in *2023 17th European Conference on Antennas and Propagation (EuCAP)*, 1–5, Florence, Italy, Mar. 2023.

[7] Bin Sayed, S., H. A. Ülkü, and H. Bağci, "A stable marching on-in-time scheme for solving the time-domain electric field volume integral equation on high-contrast scatterers," *IEEE Transactions on Antennas and Propagation*, Vol. 63, No. 7, 3098–3110, Jul. 2015.

[8] Van Diepen, P. W. N. P., M. C. v. Beurden, and R. J. Dilz, "The influence of contrast and temporal expansion on the marching-on-in-time contrast current density volume integral equation," *Progress In Electromagnetics Research B*, Vol. 104, 21–33, 2024.

[9] Pan, V. Y. and Z. Q. Chen, "The complexity of the matrix eigenproblem," in *Proceedings of the Thirty-First Annual ACM symposium on Theory of computing*, 507–516, 1999.

[10] Horn, R. A. and C. R. Johnson, *Matrix Analysis*, 2nd ed., Cambridge University Press, 2012.

[11] Wang, X., "A simple proof of descartes's rule of signs," *The American Mathematical Monthly*, Vol. 111, No. 6, 525–526, 2004.